Journal of Power Sources 194 (2009) 445–450

Contents lists available at ScienceDirect

Journal of Power Sources

journal homepage: www.elsevier.com/locate/jpowsour

Short communication

An active micro-direct methanol fuel cell with self-circulation of fuel and built-in removal of CO_2 bubbles☆

Dennis Desheng Meng*, C.J. Kim

Mechanical and Aerospace Engineering Department, University of California, Los Angeles (UCLA), 420 Westwood Plaza, Los Angeles, CA 90095-1597, USA

ARTICLE INFO

Article history:
Received 27 March 2009
Received in revised form 19 May 2009
Accepted 20 May 2009
Available online 30 May 2009

Keywords:
Micro-direct methanol fuel cell
Microfluidics
Self-circulation
Bubble pumping

ABSTRACT

As an alternative or supplement to small batteries, the much-anticipated micro-direct methanol fuel cell (μDMFC) faces several key technical issues such as methanol crossover, reactant delivery, and byproduct release. This paper addresses two of the issues, removal of CO_2 bubbles and delivery of methanol fuel, in a non-prohibitive way for system miniaturization. A recently reported bubble-driven pumping mechanism is applied to develop active μDMFCs free of an ancillary pump or a gas separator. The intrinsically generated CO_2 bubbles in the anodic microchannels are used to pump and circulate the liquid fuel before being promptly removed as a part of the pumping mechanism. Without a discrete liquid pump or gas separator, the widely known packaging penalty incurred within many micro-fuel-cell systems can be alleviated so that the system's power/energy density does not decrease dramatically as a result of miniaturization. Since the power required for pumping is provided by the byproduct of the fuel cell reaction, the parasitic power loss due to an external pump is also eliminated. The fuel circulation is visually confirmed, and the effectiveness for fuel cell applications is verified during continuous operation of a μDMFC for over 70 min with 1.2 mL of 2 M methanol. The same device was shown to operate for only 5 min if the pumping mechanism is disabled by blocking the gas venting membrane. Methanol consumption while utilizing the reported self-circulation mechanism is estimated to be 46%. Different from common pump-free fuel delivery approaches, the reported mechanism delivers the fuel actively and is independent of gravity.

1. Introduction

Because of their superior energy density, micro-direct methanol fuel cells (μDMFCs) are considered as a promising power supply for extending the operation time of portable electronics, remote sensors, and autonomous devices. Despite significant recent advancements, the development of μDMFCs has encountered serious challenges in system miniaturization. For example, within a limited space, it is difficult to accommodate all the essential components, such as the fuel delivery system, phase separator, membrane electrode assembly (MEA), interconnection components, and system housing. Also, the conventional way to remove CO_2 gas bubbles from small fuel cells is to pump them, together with the fuel, to a downstream open tank. Thus, the gas is separated from liquid by buoyancy and released to the environment. Such a separation method is orientation-dependent and subjected to liquid leakage in portable devices. The CO_2 gas bubbles cause serious clogging problems in μDMFCs [1], due to the scaling-enhanced surface tension force in the anodic microchannel. Once the microchannel of a μDMFC is blocked, the effective mass-transfer area is reduced and the cell performance will decline [2]. Therefore, parasitic power needed for the pump to remove the bubbles is relatively high. Moreover, generation of gas bubbles in the sealed anodic microchannels may elevate the pressure significantly and increase detrimental methanol crossover [3]. Existing lateral venting approaches to remove gas bubbles from microfluidic devices [4,5] are prone to leakage when the medium is methanol, especially under pressure fluctuation during operation. This problem may be addressed by employing a thin polymer membrane to allow gas diffusion [6] or designing microchannel of specific geometries to temporarily alleviate the bubble clogging [7,8]. However, producing a sufficiently high removal rate of the continuously generated gas bubbles, for a fuel cell under high loads, presents serious technical challenges.

In terms of fuel delivery, various micropumps [9–11] have been proposed to actively and precisely deliver methanol fuel for μDMFCs. However, the discrete pump is a significant source of packaging penalty for the miniaturization of fuel cells, not to mention the loss of power to run the pump. Pressurized fuel cartridges [12,13] can help deliver the fuel without power-consuming com-

☆ The manuscript has been updated and expanded from the work presented at the IEEE International Conference on Micro Electro Mechanical Systems, Kobe, Japan, January 2007.

* Corresponding author. Current address: Mechanical Engineering - Engineering Mechanics Department, Michigan Technological University, 815 R.L. Smith Building, 1400 Townsend Drive, Houghton, MI 49931, USA. Tel.: +1 906 4873551.
E-mail address: dmeng@mtu.edu (D.D. Meng).

0378-7753/$ – see front matter © 2009 Elsevier B.V. All rights reserved.
doi:10.1016/j.jpowsour.2009.05.037

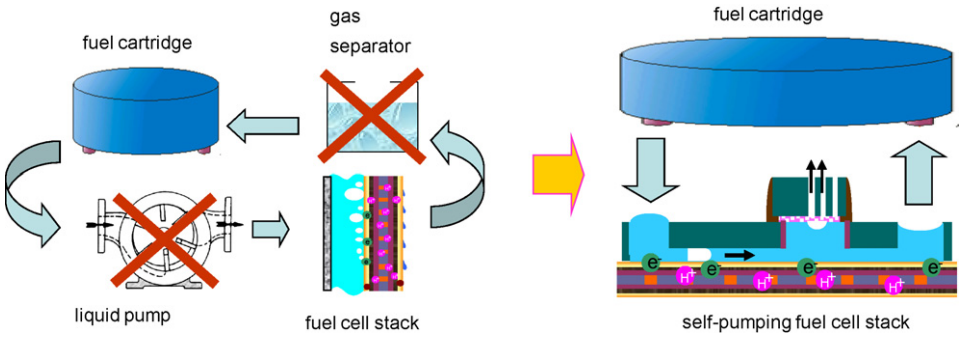

Fig. 1. It is proposed that the anode configuration can be greatly simplified for miniature fuel cells (e.g., μDMFC) by eliminating gas separator and liquid pump from the conventional configuration (shown left) and integrating the functionalities into an embedded self-circulation structure (shown right). The self-circulation mechanism has so far been proven by providing gas bubbles extrinsically through electrolysis and injection in a controlled manner [19].

ponents but cannot circulate and recycle the fuel. The pressure applied to the anodic microchannels also needs to be controlled cautiously to prevent an excessive methanol crossover. At the same time, an array of technologies has been explored to passively deliver methanol fuel to the anodic reaction chamber. Diffusion through porous media [14–16] and surface tension-induced transportation [17] present promising solutions to mix pure methanol with water and supply the mixture to the reaction chamber. However, it is difficult to achieve sufficient agitation and in situ control of fuel concentration at the reaction chamber by passive fuel delivery means. It has been proposed, although merely suggested, that the gas byproduct from the anode of a μDMFC system be fed back to the cartridge to power the fuel delivery [18]. A circulation system by buoyancy-based natural convection has also been proposed to deliver fuel without energy consumption [19]. An important advantage of pumping with reaction-generated gas bubbles is that the power generation may be automatically regulated by the external load. Higher loads induce a faster electrochemical reaction in order to generate a larger electric current. Thereby generating the CO_2 bubbles at a faster rate and accelerating the fuel circulation. However, the surface tension effect (i.e., bubble clogging) will dominate over the gravity effect (i.e., buoyancy) in a microchannel. Therefore, the performance of this natural-circulation mechanism is expected to decline with further miniaturization. Meng et al. have previously demonstrated orientation-independent venting technology to remove gas bubbles rapidly through a hydrophobic nanoporous membrane, which can tolerate pressure as high as 200 kPa for both deionized (DI) water and 10 M methanol (the highly concentrated fuel for μDMFC) [20]. Based on this technology, we developed a microchannel structure that allows a built-in liquid-pumping mechanism via directional growth and selective venting of gas bubbles. The concept has been proven with gas bubbles generated by two different means—electrolysis and gas injection [21]. In this paper, based on and expanding from [22], we verify that the CO_2 gas byproduct from the fuel-cell reaction can also be employed to pump liquid fuel and be released through the venting membrane. The microchannel structure that induces self-pumping is integrated into the anodic microchannels of a μDMFC to circulate liquid fuel with minimal packaging penalty. The parasitic energy loss by discrete micropumps is also avoided. Similar to [19], the inherent relationship between the pumping rate and the bubble generation rate is also expected to support self-regulation of fuel delivery by external electric load. Unlike [19], however, the reported mechanism does not rely on gravity effect and is therefore orientation-independent. Since the mechanism is based on the surface tension of the solid–liquid–gas interface, it will operate more efficiently in smaller microchannels, which is advantageous for miniaturization. The pumping mechanism is conceptually *embedded* into the microchannel, without calling for any multi-compartment configuration or piston components used in [18]. Differing from the passive fuel delivery approaches (e.g., [14,15,17]), the reported mechanism pumps the fuel actively, which is advantageous for fuel agitation and the reaction kinetics in microchannels. By taking advantage of the gas byproduct, which has been hindering the development of μDMFC systems, the embedded self-circulation mechanism eliminates two ancillary components simultaneously, i.e. the gas separator and the fuel pump. The system configuration on the anode side can thus be greatly simplified and seamlessly integrated, as envisioned in Fig. 1.

2. Working mechanism

The working principle of self-circulation mechanism is illustrated in Fig. 2. Based on the general bubble-pumping mechanism reported in [21], it is specifically applied to a μDMFC in this paper. The bubble pumping is accomplished by following three major, self-induced actions of the bubbles within a liquid-filled microchannel: directional growth of bubbles by the virtual check valve, directional displacement of bubbles by the hydrophilic–hydrophobic microchannel junction, and nondirectional venting of bubbles through the hydrophobic nanoporous membrane.

Let us first consider a microchannel (e.g., a glass tube) whose inner surface is wetted by the liquid (e.g., water) in hand. It is known that water can be automatically primed into a dry microchannel by capillary action. On the other hand, it takes a positive pressure to push air into the microchannel already filled with water. From the Laplace equation, the maximum pressure required to squeeze gas

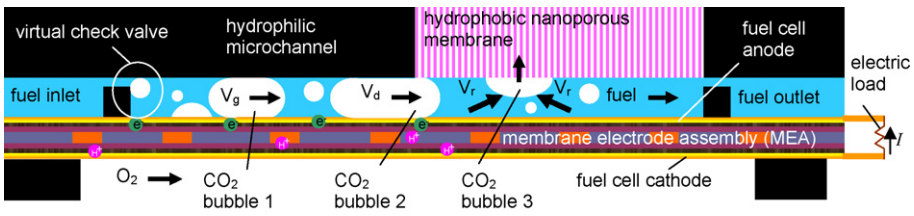

Fig. 2. Schematic description of the embedded self-circulation of liquid fuel by intrinsic CO_2 gas bubbles.

into the water-filled microchannel is calculated as

$$\Delta P^{\max} = \frac{4\sigma}{d}\cos\theta_{\text{rec}} \quad (1)$$

where σ is the surface tension of the liquid–gas interface, θ_{rec} is the receding contact angle of the liquid on the inner surface of the microchannel, and d is the hydraulic diameter of the microchannel. Since the pressure $\Delta P^{\max}$ is inversely proportional to the size of the microchannel (d), the entrance to a smaller microchannel (i.e., channel neck) may serve as an efficient virtual check valve against bubble intrusion where liquid is present. This kind of virtual check valves has been utilized for various microdevices [23–26].

Fig. 2 shows a fuel-filled microchannel with the fuel inlet on the left end and outlet on the right end, both of which are connected to a fuel cartridge via necessary additional microchannels (not shown in the figure). One set of channel necks is placed at the inlet and the other set at the outlet to regulate the flow direction, working together with the junction between hydrophilic microchannels and hydrophobic nanoporous membrane. When the fuel-cell reaction starts and CO_2 gas is generated between the two necks, a bubble will be pushed against the channel necks at the inlet. According to Eq. (1), this small gas bubble will block the leftward liquid back flow while allowing the rightward liquid forward flow. A virtual check valve is thus provided as long as the channel necks are hydrophilic. Other CO_2 bubbles inside the hydrophilic microchannel will only grow forward (i.e., to the right), pushing the liquid fuel to the right together with them. Once a bubble grows and is pushed to touch the hydrophobic part of the microchannel, the surface energy difference across the hydrophilic–hydrophobic junction induces an additional rightward displacement of the bubble. The bubble is then captured by the hydrophobic membrane and removed through its nanoscale pores selectively (i.e., gas is vented out while the liquid fuel is retained [27]). Since the bubble removal capacity of the nanoporous membrane is sufficient for the bubble generation rate in any practical μDMFC system, the virtual check valve periodically opens to take the fresh fuel in. The particular membrane we use has been proven to withstand overpressures of as high as 200 kPa for both water and 10-M methanol, fulfilling the requirement of the current, as well as next-generation μDMFCs [20]. Therefore, the directional (asymmetric) bubble growth/displacement and the nondirectional (symmetric) bubble removal will result in the net effect of a directional (forward, or rightward in the figure) pumping of the liquid fuel in the anodic microchannel. Such a directional pumping allows a fuel circulation if the fluid loop is closed for a μDMFC system. The set of channel necks at the fuel outlet is employed to prevent bubbles from accidentally entering downstream microchannels and impeding the liquid flows.

3. Device fabrication

The schematic views of the assembled self-circulating μDMFC are shown in Fig. 3. Microchannels of the anode chip, the cathode chip, and the breather cover are fabricated by deep reactive ion etching (DRIE) of a 400-μm-thick (1 0 0) silicon wafer, followed by metal evaporation (0.01 μm Cr, 3 μm Cu and 0.5 μm Au). A total of 11 microchannels are etched into the anode and cathode chips. Each channel forms a cross-section of 400 μm × 400 μm and an effective length of 11 mm. The anode and the cathode chips are then each anodically bonded to a piece of Pyrex® glass to form anode and cathode plates. A Plexiglas® fixture is then used to sandwich MEA (E-TEK®) between the anode and the cathode plates. The proton electrolyte membrane is Nafion® 117. The anode is applied with standard 4 mg cm^{-2} total metal (TM) loading using 80% high performance (HP) Pt:Ru alloy (1:1 atomic ratio) on optimized carbon. The cathode is applied with 4 mg cm^{-2} TM loading using unsupported HP Pt Black. Sufficient clamping force is required to ensure good electrical contact and to prevent fuel leakage. In order to prevent fracture of the fragile silicon chips during clamping, two silicone rubber sheets are inserted between the Plexiglas® fixture and the μDMFC device as mechanical buffer layers to distribute the clamping pressure. A piece of nanoporous polypropylene membrane (Chemplex®) is sandwiched between the anode chip and the breather cover and fixed by epoxy. The breather outlet is connected to a small mechanical manual valve (Upchurch®) via tubing. The

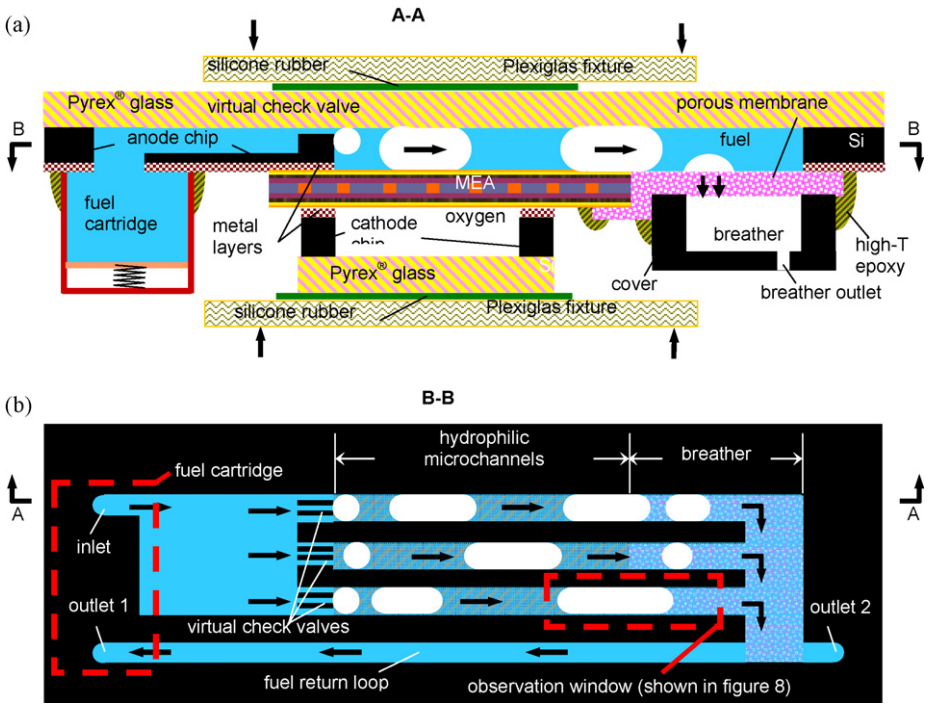

Fig. 3. Schematic drawings of the assembled self-circulating μDMFC device. (a) Cross-sectional view (A–A plane of the top view); (b) top view (B–B plane of the cross-sectional view).

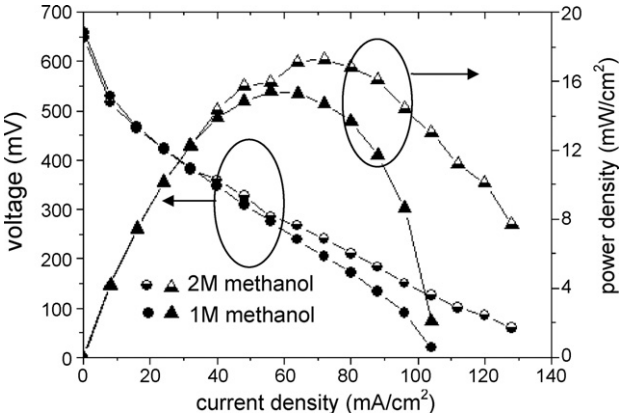

Fig. 4. Characterization of the MEA used for the μDMFC. The tests were performed under room temperature with 3 mL min^{-1} methanol flow at anode and ~100 mL min^{-1} oxygen flow at cathode.

bubble removal can be disabled to perform a control experiment by closing the valve and thus blocking the venting during the fuel-cell operation.

In order to decrease flow resistance and avoid bubble clogging, fuel inlet and fuel outlet 1 (Fig. 3b) are connected directly to a fuel cartridge, completing a fluidic loop that can be driven by the self-circulation mechanism. However, during MEA activation, water and methanol fuel should be delivered into the device and circulated by an external pump. In this case, the whole fuel cartridge is used as an inlet, and the used fuel can be discharged through fuel outlet 2. After the activation of MEA, outlet 2 will be closed, the external pump stopped, and the connection between the external pump and the fuel cartridge shut off. The fuel-cell reaction is expected to automatically start the self-pumping mechanism, circulate the fuel, and exchange it with the cartridge through inlet and outlet 1. It should be noted that the main reason for the complexity of our current device is to fabricate transparent fuel-cell devices so that we can observe and study the flows in the microchannels during fuel-cell operation. Once the principle is proven and visual characterization completed, next generation devices as well as future, practical products can adopt much simpler design and fabrication because they will not need to be transparent.

4. Activation and characterization of MEA

After assembly, the MEA of the fuel cell is activated according to the procedure provided by the manufacturer (E-TEK®). The effective active area is about 2.5 cm^2. The main purpose of the first step of the activation is to humidify the proton exchange membrane (PEM). Hot deionized (DI) water at 90 °C is first flowed through the anodic microchannels for 1.5 h with a flow rate of 3 mL min^{-1}. Then, the second step is performed to activate the catalyst, during which 2-M methanol at 80 °C is flowed through the anodic microchannels for 3 h with a flow rate of 3 mL min^{-1}. Meanwhile, oxygen is blown through the cathodic microchannel at ~100 mL min^{-1}. The cell voltage is controlled at ~250 mV by a Keithley 2425 SourceMeter® as the electrical load. During activation, an external pump (Masterflex® C/L® variable-speed tubing pump by Cole-Parmer®) is used to deliver the anodic liquid (i.e., water in the first step and 2-M methanol in the second step) from the "fuel cartridge" to the "fuel outlet 2", as shown in Fig. 3. A pressurized oxygen tank is used to flow oxygen into the cathodic microchannels. After MEA activation, the Keithley 2425 SourceMeter® is used to characterize the MEA. The tests were performed under room temperature with 3 mL min^{-1} methanol flow at anode and ~100 mL min^{-1} oxygen flow at cathode. The polarization and power density curves are shown in Fig. 4. Both 1-M and 2-M methanol solutions were tested, with the latter showing higher voltage and power output.

5. Verification of fuel circulation

In order to verify the fuel circulation, the assembled and activated μDMFC was tested with a 1.3 Ω resister as the electric load. Measurements of voltage output over time are shown in Fig. 5. When an external pump was used to deliver the 2-M methanol at a stable flow rate of 3 mL min^{-1}, the voltage output was measured to be a steady 220 mV, as expected. While using an external pump, a large external methanol source was used so that the methanol concentration remained constant over the testing time period. Then, the fuel cell was brought to self-circulation mode by closing "fuel outlet 2", turning off the external pump, and closing the connection between the external pump and the fuel cartridge. Now, the gas bubbles generated by the electrochemical reaction start to circulate the fuel in the anodic microchannels and fuel cartridge. This self-sustained fuel cell operation was observed under room temperature, with 1.2 mL of 2 M methanol in the fuel cartridge and the anodic microchannel. The cartridge and the anode were pressurized at 11 kPa over atmosphere in order to ensure rapid bubble removal through the nanoporous membrane. The pressure was equally applied to both the inlet and the outlet of the anode microchannels. It was observed that the liquid flow stopped immediately when the external circuit was disconnected, while the pressure was still applied. This verified that the pressure did not contribute to fuel circulation. Rather, the pressure helps removing the bubbles when the total volume of the liquid decreases towards the end of the fuel cell operation. The fluctuation observed in the current output during the first 20 min is likely due to the bubbles trapped in certain parts of the microfluidic loop. After this transient period, a relatively stable current output, which is comparable to the top reference case obtained with an external pump (~167 mA), was observed until the voltage started to drop gradually (at ~60 min) as the fuel was

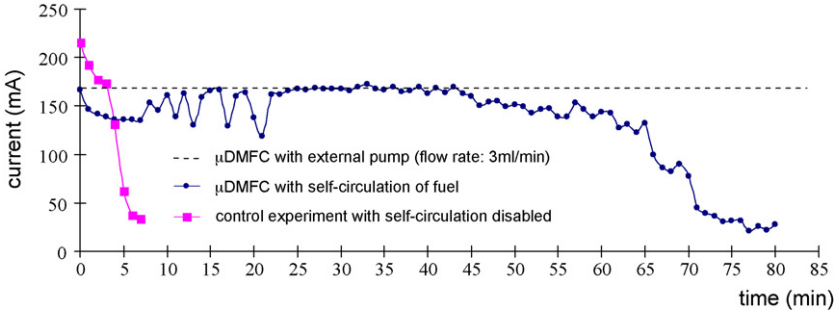

Fig. 5. Self-circulation mechanism is verified by measuring the current output of a given μDMFC device under three different scenarios for fuel delivery. The device operated over 70 min with the self-circulation of fuel, while it lasted less than 5 min with the self-circulation disabled (i.e., under passive operation). The device operation with an external fuel pump delivering an unlimited amount of fuel is shown as a top reference.

used up. The following equation is used to estimate the methanol utilization (Faraday efficiency):

$$\eta = \frac{\int I\ dt}{6CVF} \times 100\% \quad (2)$$

where C and V are the concentration (2 M) and volume (1.2 mL) of the methanol solution, respectively, F is the Faraday constant (9.65×10^4 C mol^{-1}); and $\int I\,dt$ is the total charges extracted from the fuel during discharging (1.07×10^4 mA min = 642 C). The methanol utilization under the reported self-circulation mechanism is therefore estimated to be 46.2%, which is very close to the value reported in the literature (49.7% for 2 M methanol) [28].

The fuel cell operation over a considerable time span (over 70 min) indicated that the fuel was indeed circulated by the proposed self-pumping mechanism. As a bottom reference, an experiment was performed by closing the valve connected to the breather outlet. The venting of CO_2 bubbles was thus blocked to disable the self-circulation mechanism. In this passive mode, we observed gas bubbles growing and filling the entire anodic microchannel and power output dropped rapidly after about 3 min. The oxygen flow in the cathodic microchannel was kept at ~53 mL min^{-1} for all testing modes.

The anodic microchannels in the tested μDMFC were made transparent to allow a visual confirmation of fuel circulation and detailed observation of flows for future improvement. A bubble displacement pattern similar to that in [21] has been observed throughout the flow field, confirming the pumping mechanism we had envisioned. Fig. 6 demonstrates the bubble motion near the end of an anodic microchannel, as well as the successful bubble removal. We also observed that the speed of bubble motion increased along the microchannel (left to right in Fig. 2 or Fig. 3). The self-circulation mechanism also holds the potential to be self-regulated by the fuel cell load. Regulation of the flow rate by the bubble generation rate has been observed in a similar pump-loop driven by electrolysis [21]. Expecting that the flow rate in the μDMFC (i.e., fuel delivery rate) is also regulated by the bubble generation rate, which is autonomously determined by the external electric load, we envision a device whose power generation can be self-regulated by the applied loading. Ye et al. [19] has experimentally verified self-regulation of their buoyancy-driven fuel delivery system, which also employed the CO_2 bubbles generated by fuel-cell reaction.

A limitation on the current μDMFC device is the need to keep the anodic microchannels at pressures above atmosphere to ensure rapid gas removal, which may introduce additional crossover. We used 11 kPa in our tests, an arbitrary value, to satisfy the venting need of the given test device. When the pores of the venting membrane and the venting section in the microchannels are optimized in the future, we expect that the required pressure will be decreased. Further research is expected to reduce the anodic pressure so that it can be comparable to or lower than that produced by an external pump or pressurized fuel cartridge.

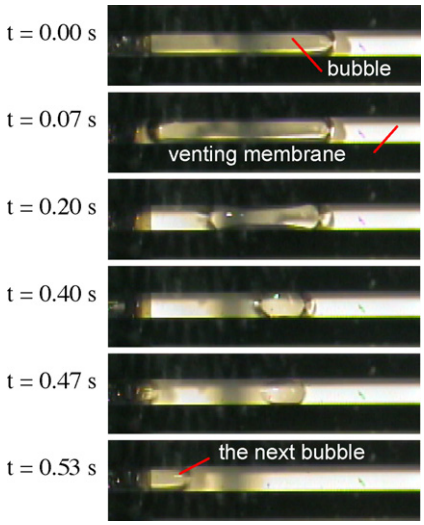

Fig. 6. A sequence of video frames shows a CO_2 bubble being removed through the breather (i.e., nanoporous venting membrane).

6. Discussion: balance of plant for μDMFC

A major limiting factor in the development of μDMFC is methanol crossover, which not only leads to fuel waste but also produces mixed potential [29–31]. The voltage output is thus decreased, and the energy and power density of the μDMFC system significantly reduced. Over the past decades, great research efforts have been devoted to develop new PEMs with high methanol resistance to reduce crossover [32–35]. However, the low-crossover PEM technology is far from mature today. The typical maximum fuel concentration of μDMFC is still much lower than 10 M, which means that over 60 vol.% of the fuel in the anodic reaction chamber should be water. Obviously, carrying highly diluted fuel in the μDMFC fuel cartridge will greatly diminish the system's energy density. On the other hand, the fuel-cell electrochemical reactions have provided a clue to a potential solution. For every one water molecule consumed at the anode ($CH_3OH + H_2O \rightarrow 6e^- + 6H^+ + CO_2\uparrow$) three water molecules will be generated at the cathode ($1.5O_2 + 6e^- + 6H^+ \rightarrow 3H_2O$). Therefore, the fuel-cell reaction at the cathode can generate enough water to dilute the fuel in the anodic chamber and supply the reaction. If the water from the cathode can be recycled and mixed with pure methanol from the cartridge, even the current PEM technology may provide a μDMFC with much higher energy density.

As described in Section 1, another practical issue to be resolved in a μDMFC is the intrinsically generated CO_2 gas bubbles. In a large-scale stationary direct methanol fuel cell, the gas bubbles can be pumped together with the used fuel to a gas separator, essentially an open tank, where bubbles are released. The performance of the system is not affected significantly by gas generation. However, in a μDMFC the tiny CO_2 gas bubbles cause serious bubble clogging problems so that the effective mass-transfer area is reduced, parasitic power loss is increased, and the methanol crossover effect deteriorates.

Since problems such as methanol crossover and gas bubble removal are usually coupled with each other, the solution has to be considered on the system level, with an essential *balance of plant* components to handle reactants and byproducts of μDMFCs efficiently. Various system configurations [36] have been proposed for μDMFCs. Passive configurations are always attractive for these small power generators because elimination of active components reduces both the volume ratio of inactive material (i.e., packaging penalty) and parasitic energy losses. These effects become more significant as the system becomes smaller because the volume and energy consumption of active components remain relatively constant even though the reactants and the total energy available in the system are reduced. To give an example of the simplest configurations, a μDMFC system without active components is shown in Fig. 7a with the anode completely immersed in the fuel reservoir and cathode directly opened to the air [37]. In spite of its potential advantages for small applications, all the factors that limit the performance of μDMFC systems remain challenging in such a configuration. Diluted fuel (e.g., 5 M or 20 vol.%) has to be used to reduce methanol crossover and CO_2 gas bubbles remain in the fuel reservoir. Also, removal of water byproduct from the cathode relies on natural evaporation. In addition, the performance of the system under the unpredictable operation conditions of practical applica-

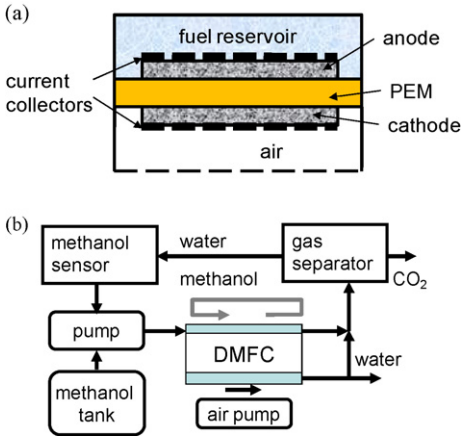

Fig. 7. Two exemplary configurations for μDMFC systems. (a) A completely passive system (drawn according to [37]); (b) A completely active system (drawn according to [38]).

tions can be further undermined, provided that no mechanism is designed to regulate the system according to the variable operation conditions. On the other hand, relatively large DMFC systems tend to adopt a completely active configuration [9,38], as Fig. 7b illustrates. A liquid pump is used to recycle the used fuel from the anodic chamber, mix it with the water recovered from cathodic chamber and the pure methanol from the fuel tank, and then feed the fuel back to the anodic chamber. The optimum fuel concentration can be obtained according to the operation conditions under the control of a fuel concentration regulation system, including the methanol sensor and the relevant electronic circuit. The CO_2 byproduct is removed through the gas separator. An air pump or fan is employed to deliver oxygen to the cathode. Completely active configurations can provide optimum performance at the cost of complex auxiliary components and the associated parasitic power loss, which usually cannot be afforded in a μDMFC system.

It would be ideal if the advantages of passive and active approaches can be combined by employing a series of integrated passive components that can fully or partially realize active reactant handling and regulation functionalities. In this paper, we have provided an example of such a balance of plant components on the anodic side of μDMFC system, so as to provide a basis for the further realization of similar functionalities on the cathode side and eventually the whole system.

7. Conclusions

An embedded self-circulation structure is integrated into a μDMFC to actively deliver liquid fuel to the anode microchannel and agitate the fuel without any discrete power-consuming pumping component. The structure also achieves orientation-independent gas removal, without introducing an additional gas separator. Simultaneous elimination of the two ancillary components (i.e., the gas separator and the liquid pump) will greatly reduce the packaging penalty and increase the ratio of active material as well as the energy and power density of the system. Without the external fuel pump, parasitic power loss on fuel delivery can be avoided, so that the total efficiency of the system can be improved. The self-circulation mechanism also holds the potential to regulate the reaction autonomously per the electric load without any control circuit. The fuel circulation has been verified by continuous operation of the system for over 70 min, as well as visual confirmation. The proposed mechanism provides an anode-side example for passive balance of plant components for the next-generation μDMFCs.

Acknowledgements

This work was supported by the Defense Advanced Research Projects Agency (DARPA) Micro Power Generation (MPG) Program and the UCLA Faculty Research Grant. The authors wish to thank Professors C.-M. Ho, C.Y. Wang, X. Zhang, X. Zhong, T. Cubaud, T.J. Yen, as well as Drs. G.Q. Lu and M. Tatineni for their valuable discussions, Dr. Y.M. Tsou at BASF Fuel Cells, Inc. for the discussions and technical information on MEA, and Ms. A. Lee, Mr. R. Lemmens, and Mr. B. Van Dyk for their editorial assistance.

References

[1] G.Q. Lu, C.Y. Wang, J. Power Sources 134 (2004) 33–40.
[2] C.W. Wong, T.S. Zhao, Q. Ye, J.G. Liu, J. Electrochem. Soc. 152 (2005) A1600–A1605.
[3] M. Hogarth, in: G. Hoogers (Ed.), Fuel Cell Technology Handbook, CRC Press LLC, Boca Raton, FL, 2003.
[4] J.-H. Tsai, L. Lin, Sens. Actuators A 97–98 (2002) 665–671.
[5] Z. Yang, S. Matsumoto, R. Maeda, Sens. Actuators A 95 (2002) 274–280.
[6] S. Prakash, W.E. Mustain, P. Kohl, ECS Meeting Abstracts 702 (2007) 605–1605.
[7] J. Kohnle, G. Waibel, R. Cernosa, M. Storz, H. Ernst, H. Sandmaier, T. Strobelt, R. Zengerle, Proceedings of the IEEE International Conference on Micro Electro Mechanical Systems, Las Vegas, NV, January, 2002, pp. 77–80.
[8] C. Litterst, S. Eccarius, C. Hebling, R. Zengerle, P. Koltay, J. Micromech. Microeng. (2006) S248.
[9] C. Xie, J. Bostaph, J. Pavio, J. Power Sources 136 (2004) 55–65.
[10] T. Zhang, Q.-M. Wang, J. Power Sources 140 (2005) 72–80.
[11] C.R. Buie, D. Kim, S. Litster, J.G. Santiago, Electrochem. Solid-State Lett. 10 (2007) B196–B200.
[12] S.-C. Yao, X. Tang, C.-C. Hsieh, Y. Alyousef, M. Vladimer, G.K. Fedder, C.H. Amon, Energy 31 (2006) 636–649.
[13] R. Luharuka, C.-F. Wu, P.J. Hesketh, Sens. Actuators A 112 (2004) 187–195.
[14] Z. Guo, Y. Cao, J. Power Sources 132 (2004) 86–91.
[15] Z. Guo, A. Faghri, J. Power Sources 160 (2006) 1142–1155.
[16] A. Oedegaard, C. Hentschel, J. Power Sources 158 (2006) 177–187.
[17] Y. Yang, Y.C. Liang, J. Power Sources 165 (2007) 185–195.
[18] G.C. McNamee, W.P. Acker, US Patent No. 6,699,021.
[19] Q. Ye, T.S. Zhao, J. Power Sources 147 (2005) 196–202.
[20] D.D. Meng, T. Cubaud, C.-M. Ho, C.-J. Kim, J. Microelectromech. Syst. 16 (2007) 1403–1410.
[21] D.D. Meng, C.-J. Kim, Lab Chip 8 (2008) 958–968.
[22] D.D. Meng, C.-J. Kim, Proceedings of the IEEE International Conference on Micro Electro Mechanical Systems, Kobe, Japan, January, 2007, pp. 85–88.
[23] F.-G. Tseng, C.-J. Kim, C.-M. Ho, J. Microelectromech. Syst. 11 (2002) 427–436.
[24] F.-G. Tseng, C.-J. Kim, C.-M. Ho, J. Microelectromech. Syst. 11 (2002) 437–447.
[25] X. Geng, H. Yuan, H.N. Oguz, A. Prosperetti, J. Micromech. Microeng. 11 (2001) 270–276.
[26] N.R. Tas, J.W. Berenschot, T.S.J. Lammerink, M. Elwenspoek, A.v.d. Berg, Anal. Chem. 74 (2001) 2224–2228.
[27] D.D. Meng, J. Kim, C.-J. Kim, J. Micromech. Microeng. 16 (2006) 419–424.
[28] Q.-Z. Lai, G.P. Yin, Z.B. Wang, C.Y. Du, P.J. Zuo, X.Q. Cheng, Fuel Cells 8 (2008) 399–403.
[29] D. Chu, S. Gilman, J. Electrochem. Soc. 141 (1994) 1770–1773.
[30] Z. Jusys, R.J. Behm, Electrochim. Acta 49 (2004) 3891–3900.
[31] W. Li, S. Song, W. Zhou, G. Sun, Q. Xin, C. Poulianitis, P. Tsiakaras, Ionics 11 (2005) 112–119.
[32] A. Heinzel, V.M. Barragan, J. Power Sources 84 (1999) 70–74.
[33] Y.H. Pan, Electrochem. Solid-State Lett. 9 (2006) A349–A351.
[34] A. Yamauchi, T. Ito, T. Yamaguchi, J. Power Sources 174 (2007) 170–175.
[35] Y. Si, J.-C. Lin, H.R. Kunz, J.M. Fenton, J. Electrochem. Soc. 151 (2004) A463–A469.
[36] W. Qian, D.P. Wilkinson, J. Shen, H. Wang, J. Zhang, J. Power Sources 154 (2006) 202–213.
[37] D. Kim, E.A. Cho, S.-A. Hong, I.-H. Oh, H.Y. Ha, J. Power Sources 130 (2004) 172–177.
[38] K. Yoshida, Y. Hagihara, S. Tanaka, M. Esashi, Proceedings of the IEEE International Conference on Micro Electro Mechanical Systems, Istanbul, Turkey, January, 2006, pp. 722–725.